Lab Report 3: X-Ray Spectroscopy

By **Sean Alexander**, lab conducted with Cathal Maguire

January 2024

Contents

1 Abstract

In the following experiments, X-ray spectrum of molybdenum were investigated at different accelerating voltages, revealing distinct transitions, including K_α and K_β. Analysis of the data yielded a product of $U \cdot \lambda_{\text{min}}$ which aligned with the hypothesis that it is constant, with an average value of $\approx 1.15\,\mu m \cdot V \cdot \text{Å}$. The calculated values for Planck's constant exhibited good agreement with the accepted value, with an average of $\approx 6 \times 10^{-34}\,\text{J} \cdot \text{s}^{-1}$. Furthermore, the experiment confirmed Mosley's Law by determining a proportionality for K-edge energies for various metal foils and estimate Rydberg's constant to be 10μm. The absorption coefficients and mass attenuation coefficients demonstrated clear dependence on atomic number Z, highlighting the effectiveness of X-ray spectroscopy in material analysis.

2 Theory and Introduction

X-Ray Spectroscopy is a method used in material analysis to determine the chemical composition and crystal structure of materials. X-ray spectra, and scattering & absorption mechanics are an important concepts in understanding X-ray spectroscopy.

2.1 X-Ray Spectra

An X-ray spectrum of a material consists of a plot of the wavelength of the emitted photons upon bombarding the target with electrons against the absolute or relative intensity of the emitted radiation.

Shown below is an X-Ray spectrum of molybdenum:

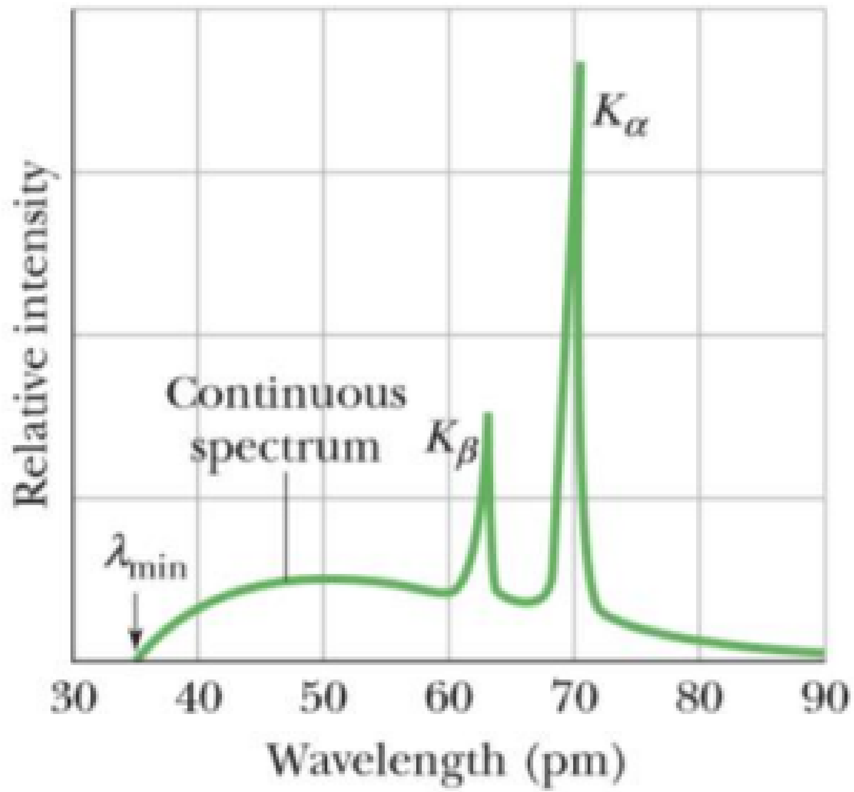

Figure 1: *X-Ray Spectrum of Molybdenum*

The X-ray spectrum of molybdenum is made up in part by the continuous spectrum which is derived from the photon emission produced by the deceleration of incident electrons upon striking it.

There is a minimum associated wavelength λ_{min} in the continuous spectrum which can be determined if one equates the work done by the accelerating voltage and energy of the emitted X-ray as the electron cannot lose more kinetic energy than the value that its acceleration allows. This is shown below:

$$\text{Emmited Photon Energy} = \text{Voltage Work} \tag{2.1}$$

$$\therefore \frac{h \cdot c}{\lambda_{min}} = e \cdot U \tag{2.2}$$

$$\rightarrow \lambda_{min} = \frac{h \cdot c}{e \cdot U} \tag{2.3}$$

The remaining component of the X-ray spectrum is known as the characteristic spectrum. The characteristic spectrum corresponds to the radiation emitted due to the energy state transitions which occur when an electron in a high energy state replaces a displaced electron with a lower energy state removed from an orbital of an atomic component the material subjected the bombardment. This consists of peaks which correspond to the wavelengths and intensities of the characteristic energy state transitions of the subjected material.

In the case of molybdenum, the peaks are associated with the energy state transitions K_α & K_β. These are the transitions associated with electrons transitioning to principal quantum number $n = 1$ from $n = 2\,\&\,3$ respectively.

In order to give an estimate of the energies of the X-rays emitted during these energy level transitions, one may use a modified version of the Bohr Model of the binding energy of an electron adjusted to account for the "screening effect". The "screening effect" can be expressed as where electrons of lower energy states can be viewed to be decreasing the binding energy of electrons in the atom's higher energy levels due to the presence of their charge lowering the effective charge of the nucleus. This modified Bohr model is expressed below:

$$E_n = -\frac{R \cdot h \cdot c \cdot Z_{eff}^2}{n^2} \tag{2.4}$$

Where:

$$R = \frac{\mu_0^2 \cdot m_e^4 \cdot c^3}{8h^3},\ Z_{eff} = Z - \sigma_m \tag{2.5}$$

Where R is the Rydberg constant, h is planks constant, c is the speed of light in a vacuum, Z_{eff} is the effective atomic number of the nucleus, μ_0 is the permeability of free space, m_e is the mass of an electron, Z is the atomic number of the nucleus, and σ_m is the "screening constant" which for the purposes of this estimate was taken to be equal to the half the number of electrons in the lowest principal quantum state after the transition. This is an appropriate estimate for the type of transitions under investigation as each electron is seen to negate half an e of charge, as they are probably not occupying the exact same space as the nucleus at any given time.

For the K_α transition, the difference in estimated binding energy of the electron before and after the transition, and thus the estimate for the photon energy is:

$$E_{K_\alpha} = E_2 - E_1 = -\frac{R \cdot h \cdot c \cdot Z_{eff}^2}{(2)^2} + \frac{R \cdot h \cdot c \cdot Z_{eff}^2}{(1)^2} \tag{2.6}$$

Where:

$$R = \frac{\mu_0^2 \cdot m_e^4 \cdot c^3}{8h^3},\ Z_{eff} = (42) - (1) \tag{2.7}$$

This results in $E_{K_\alpha} = R \cdot h \cdot c \cdot \frac{5043}{4}$ or $E_{K_\alpha} \approx 17$ keV.

This was then repeated for the energy of the photon associated with the K_β transition:

$$E_{K_\beta} = E_3 - E_1 = -\frac{R \cdot h \cdot c \cdot Z_{eff}^2}{(3)^2} + \frac{R \cdot h \cdot c \cdot Z_{eff}^2}{(1)^2} \tag{2.8}$$

Where

$$R = \frac{\mu_0^2 \cdot m_e^4 \cdot c^3}{8h^3},\ Z_{eff} = (42) - (1) \tag{2.9}$$

This results in $E_{K_\beta} = R \cdot h \cdot c \cdot \frac{1348}{9}$ or $E_{K_\beta} \approx 20$ keV.

These estimates for E_{K_α} and E_{K_β} align with values achieved by Lawrence Berkeley National Laboratory which were $E_{K_{\alpha_1}}, E_{K_{\alpha_1}} = 17.47934, 17.3743$ keV, and $E_{K_\beta} = 19.6083$ keV. These experimentally achieved results align with the estimations derived using the modified Bohr model to two significant figures, thus lending credence to the estimation method's viability and establishing an associated radius of error for future estimations of this kind.

The energies of these transitions emitted X-rays are discrete and unique to their characteristic elements which is the basis of the method of X-ray fluorescence (XRF) which is a method used to determine which elements are present in a solid sample.

For the purpose of studying large, solid crystal structures, Bragg's Law is used to determine the crystals properties. Bragg's Law is Included below:

$$2d \cdot sin(\beta) = n \cdot \lambda \tag{2.10}$$

Where d in the crystal's inter-planar spacing or distance, n is the integral diffraction order, β is the angle of diffraction/ constructive interference measured as the angle of incidence against the horizontal, and λ is the wavelength of the diffracted light.

2.2 X-Ray Absorption & Scattering

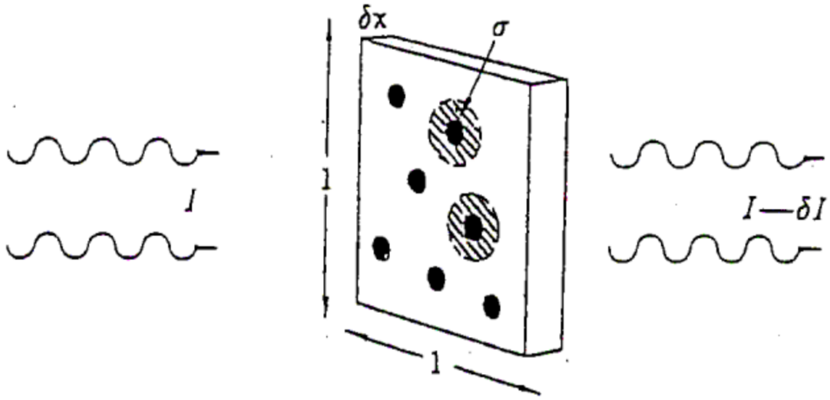

Figure 2: *Thin homogeneous Slab with Incident Radiation*

Given a thin homogeneous slab with a radiation of intensity I incident upon it, with atoms of cross-sectional area σ, and a number density of n atoms per unit volume, and additionally assuming that every photon incident on the cross-sectional area of any given atom is either absorbed or scattered, one may determine the following:

$$\text{Proportional Change in Intensity} = \text{Product of Slab Number Density and Volume} \tag{2.11}$$

$$\therefore \frac{-\delta I}{I} = n \cdot \sigma \cdot \delta x \tag{2.12}$$

$$\rightarrow \int_{I_0}^{1} -\frac{1}{I}\,\delta I = \int_{0}^{x} n \cdot \sigma \cdot \delta x \tag{2.13}$$

$$\rightarrow I = I_0 \cdot e^{-\mu \cdot x} \tag{2.14}$$

Where I is the intensity of the incident light, and μ is the linear attenuation coefficient which is equivalent to $n \cdot \sigma$, and x is the thickness of the slab.

The atomic cross-sectional area σ and the removal cross-section are equivalent, and the atomic number density n is equivalent to the product of Avogadro Number N_a and the ratio of the material density ρ and the atomic mass A as indicated below:

$$n = N_a \cdot \frac{\rho}{A} \tag{2.15}$$

Therefore the removal cross-section σ can be expressed as shown below:

$$\sigma = \frac{\mu}{n} = \frac{\mu \cdot A}{\rho \cdot N_a} \tag{2.16}$$

The ratio of the linear attenuation coefficient μ and the material density ρ is known as the mass attenuation coefficient and is equivalent to the fraction of photons removed from a radiation source by the thin homogeneous slab per unit mass.

Assuming there are two distinct regions of the removal cross-section σ which are primarily responsible from the absorption and scattering of the incident radiation, being σ_a and σ_s respectively, one must conclude the following:

$$\sigma = \sigma_a + \sigma_s \tag{2.17}$$

Where σ_a, and σ_s are the 'partial' cross-sections associated with absorption and scattering respectively.

X-rays with associated energies 10 - 40 keV which is the energy range this experiment is primarily concerned with are primarily absorbed by the mechanics the photoelectric effect. This process converts the photon energy such that a bound electron of the material is ejected. Generally electrons with lower energy states contribute the most to this process but in the case of the ejection of "K" energy level electrons, the following must be true:

$$h \cdot \nu \geq E_1 = E_k \tag{2.18}$$

One may then conclude that there is therefore an acute increase in photoelectric cross-section (and therefore in attenuation) occurring when incident photon energy reaches this binding energy. This is illustrated below:

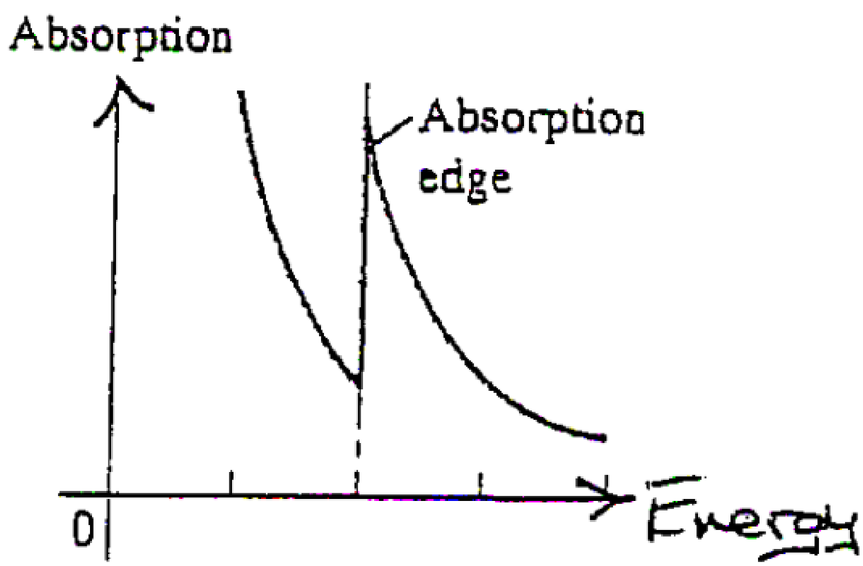

Figure 3: *Diagram Identifying the Absorption Edge in the Absorption-Energy Plot of a Solid*

For the k or 1^{st} energy level the discontinuity is called the K-edge and at this incident photon energy the following is true:

$$E_k = \frac{h \cdot c}{\lambda_k} = R \cdot h \cdot c \cdot (Z - \sigma_K)^2 \tag{2.19}$$

Where σ_K is K energy-level screening parameter.

This equation aligns with the empirical relation found by Henry Moseley in 1913:

$$\sqrt{\frac{1}{\lambda K}} \propto (Z - \sigma_K)^2 \tag{2.20}$$

There may also be edges for other energy levels. If one selects a material with an edge at a suitable energy, it is possible to filter out the higher energy K_α edge to delineate the lower energy K_β line whilst minimally attenuating it.

As the photon energy increases, along the plot shown in Figure 3, there is a sharp decrease in absorption after the discontinuity. Additionally, at a fixed energy separation from an edge, the absorption cross-section σ_a increases rapidly proportional to the atomic number Z of the absorbing atom. In the following experiments, this relationship will be taken as quartic:

$$\sigma_a \propto Z^4 \tag{2.21}$$

The theory discussed above is relevant to the experiments described below.

3 Apparatus

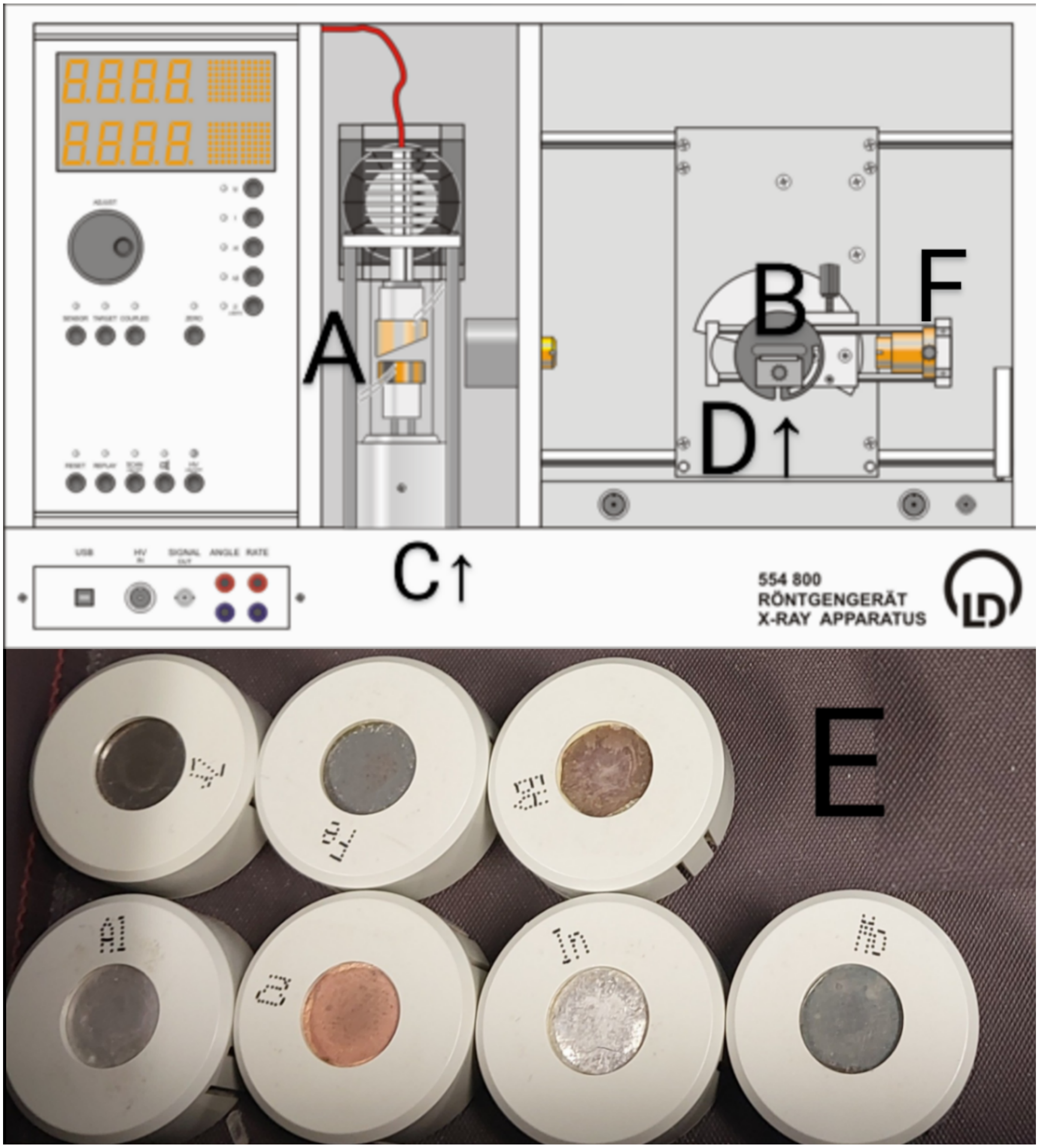

Figure 4: *The Apparatus*

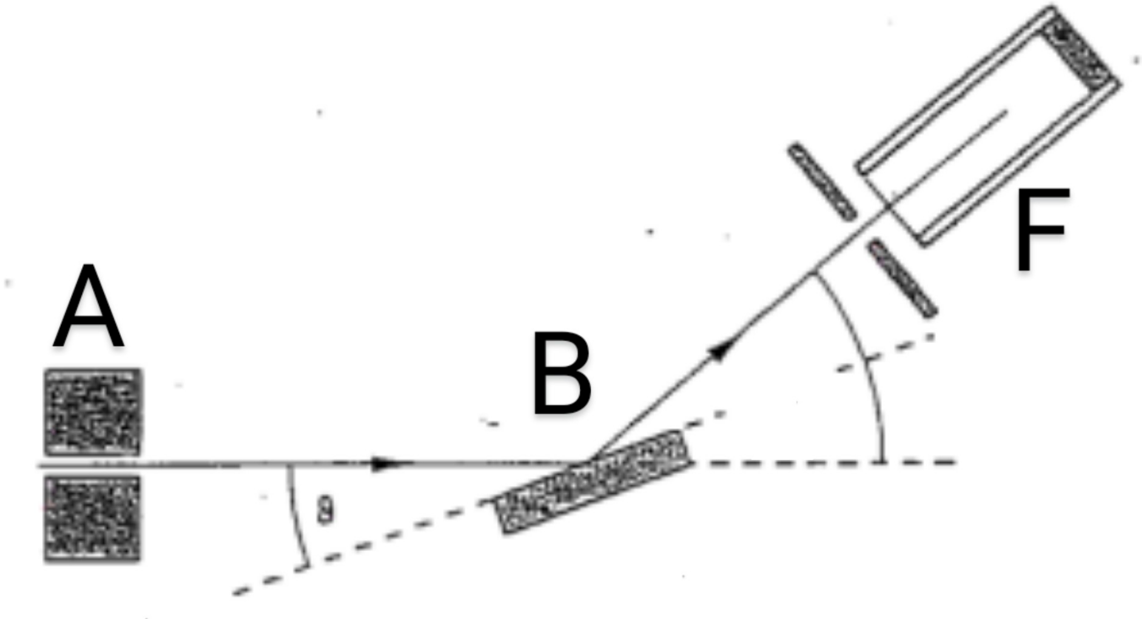

Figure 5: *The Apparatus Schematic Diagram*

The apparatus associated with this experiment includes:

- A: Collimator and X-ray tube with Molybdenum anode.
- B: Monocrystal slab of (1 0 0) NaCl
- C: Leaded Glass (Door must be shut as X-rays are emmited)
- D: Goniometer which adjusts the angle of incidence of X-Rays
- E: Attenuating metal foils including: Al, Fe, Cu, Zr, Mo, Ag, In with parameters detailed in Figure 4
- F: Counter Tube
- Lens cleaning tissues
- Calipers
- Gloves
- PC with associated counting software

Foil	Z	A	Thickness (mm)	Density (kgm^{-3})
Al	13	26.98	0.5	2698
Fe	26	55.84	0.5	7873
Cu	29	63.54	0.07	8933
Zr	40	91.22	0.05	6507
Mo	42	95.94	0.1	10222
Ag	47	107.87	0.05	10500
In	49	114.82	0.3	7290

Figure 6: *Metal Foil Parameters*

The leaded glass door must be shut before any measurement is made.

The NaCl crystal must be gently cleaned before measurements with lens cleaning tissue to avoid contamination.

The NaCl crystal should be handled by its edges rather than its faces to avoid shattering.

All manipulation of materials should be undergone through the spectroscopes control panel.

4 Methodology

4.1 Experiment 1:

The aims of **Experiment 1** include:

1. To record the X-ray spectrum of molybdenum at different accelerating voltages.
2. To show that $U \cdot \lambda_{min}$ is a constant, and to use this to estimate Planck's constant h.
3. To measure the photon energies (and wavelengths) lines of the K_α, and K_β in the characteristic spectrum of molybdenum and to compare these with values calculated using theory.

In order to achieve the goals outline above:

- The X-rays were dispersed into their spectrum by diffracting them using the (1 0 0) NaCl crystal using the Bragg geometry.
- This was achieved through installing the NaCl crystal on the goniometer and screwing it in place gently.
- The orientation which gives the greatest intensity was found through determining the intensity for small values of Δt and varying for the best intensity by trial and error (U = 35kV, I =1 mA). Increasing Δt for higher resolution afterwards ($\Delta\beta = 0.1$).
- Coupled was selected on the detector such that it is rotated twice the angle of rotation of the sample as is required for the Bragg geometry and limits of 3 and 10 were selected.
- Scan was pressed in order to obtain a graph of the intensity I against the angle β

- Bragg's Law (**Equation 2.10**) was used under the assumption that the order n was equal to 1 and the inter-planar spacing or distance d was equal to 281.5 [pm] to be able to note the associated wavelength given every angle β.
- To determine whether $U \cdot \lambda_{min}$ is a constant, the measurements were repeated for U values of 30, 25 & 20 kV, and these spectra were then displayed simultaneously on the software.
- From these spectra, the values of the minimum wavelength λ_{min}, the wavelengths of the K_α and K_β transition lines were then found.
- These values were then used to determine the associated emitted photon energies which are E_{max}, E_{K_α}, and E_{K_β} respectfully.
- The product $U \cdot \lambda_{min}$ was then calculated and it was determined whether or not it was a constant under different input voltages U.
- The energies $E_{\lambda min}$, $E_{\lambda K_\alpha}$, and $E_{K\beta}$ were then estimated (**Equation 2.19**) using the achieved data and compared to theoretical values calculated using the modified Bohr model (**Equation 2.4**). They were then compared.

4.2 Experiment 2:

This experiment includes two sections. **Section 1** revolves around the K-absorption edge, while **Section 2** is concerned with the absorption of X-rays at a fixed wavelength from the edge.

The aims of **Experiment 2 - Section 1** include:

1. To determine the energy E_K of the K-absorption edge for zirconium (Zr), molybdenum (Mo), silver (Ag) and indium (In) metal foils.
2. To show that Mosley's Law: $E_k \propto (Z - \sigma_K)^2$ (**Equation 2.20**) is true
3. To estimate the Rydberg constant R and the value of σ_K

The aims of **Experiment 2 - Section 2** include:

1. To estimate the mass attenuation coefficient ($\mu \cdot \rho$), and absorption coefficient (σ_a) for Aluminium (Al), Iron (Fe), Copper (Cu) and Zirconium (Zr) metal foils at a fixed wavelength away from the absorption edges (being ≈ 41 [pm])
2. To determine the dependence of the absorption coefficient σ_a on the atomic number Z at this wavelength.

4.2.1 Experiment 2 - Section 1:

In order to achieve the goals outline above for this section:

- In order to determine the the K-edge in the metals listed above, the X-ray spectrum of molybdenum with and without the metal foils listed above were inserted into the X-Ray output. (The NaCl crystal was again used to disperse the spectrum)
- An angle (β) range of 3 to 12 was selected and the spectrum of the spectrum ($\frac{R_0}{\lambda}$) without a metal foil covering the exit slit was achieved.
- Following from this, the spectra with the metal foils of zirconium, molybdenum, silver and indium were achieved.

- The data associated with the aforementioned spectra superimposed upon each-other and the transmittance ($\frac{T}{\lambda}$) spectra were noted.
- The count rate (R) of the metal foils was then divided by the count rate of the spectra without the foils and these spectra were compared to the programme generated transmission data as $T = \frac{I}{I_0} = \frac{R}{R_0}$.
- The values of the wavelengths (λ_{K}), the transmittance values (T_{K}), and the photon energies (E_{K}) associated for "K-edges" were then discerned and tabulated.
- The transmittance per wavelength ($\frac{T}{\lambda}$) data, and the relation $\sigma_{\mathrm{K}} = \frac{ln(T_{\mathrm{K}})}{x \cdot \rho}$ was then use to plot the ratio of the K-edge energy (E_{K}) to the calculable quantity $h \cdot c \cdot (Z - \sigma_{\mathrm{K}})^2$ to demonstrate Mosely's law and estimate the Rydberg constant using the slope.

4.2.2 Experiment 2 - Section 2:

In order to achieve the goals outline above for this section:

- In order to measure the attenuation a fixed wavelength away from the absorption edge such that data was measurable but not too close to the edge was selected and noted and tabulated in each case.
- The count rate at these points were then noted and tabulated without a metal foil and with Aluminium, Iron, Copper, and Zirconium foils covering the slit.
- This was then repeated to find an additional count rate data selection.
- The data was then used to determine to the values of the absorption cross section assuming the scattering cross-section was equivalent to $0.02A \cdot N_a^{-1}$ and noting that: $\sigma_{\mathrm{a}} = \frac{ln(T_{\mathrm{K}}^{-})}{x} - \sigma_{\mathrm{s}}$

5 Data

5.1 Experiment 1:

Included below is the data achieved in this experiment:

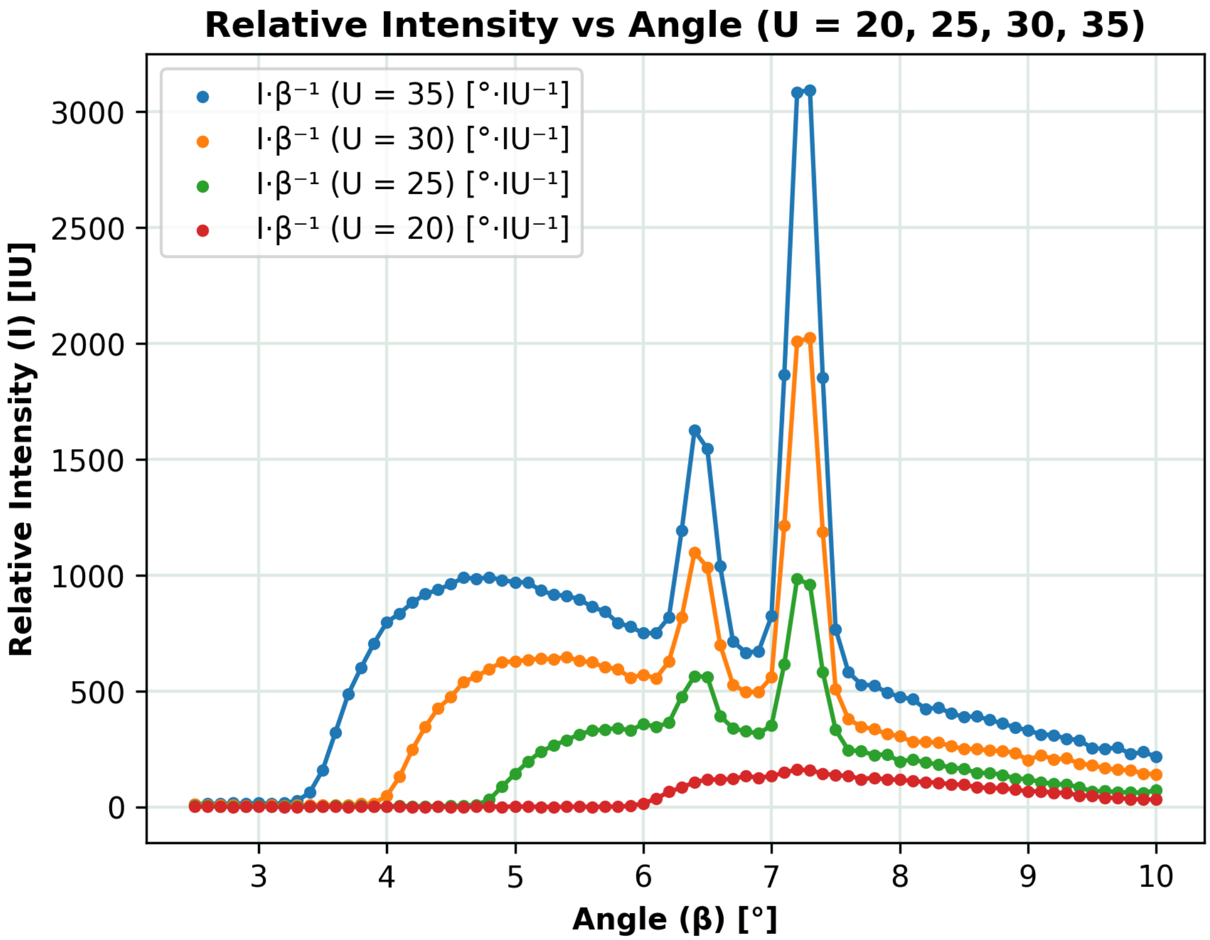

Figure 7: *Experiment 1: Data*

Accelerating Voltage (U) [$\pm$0.1 kV]	**Minimum Angle** $(\beta_{\lambda_{min}})$ [$\pm$0.5]	K_β **Transition Angle** (β_{K_β}) [$\pm$0.5]	K_α **Transition Angle** (β_{K_α}) [$\pm$0.5]
20	5.9	6.6	7.2
25	4.7	6.4	7.2
30	3.8	6.4	7.3
35	3.3	6.4	7.3

Table 1: Experiment 1: Numerical Data

5.1.1 Experiment 2 - Section 1:

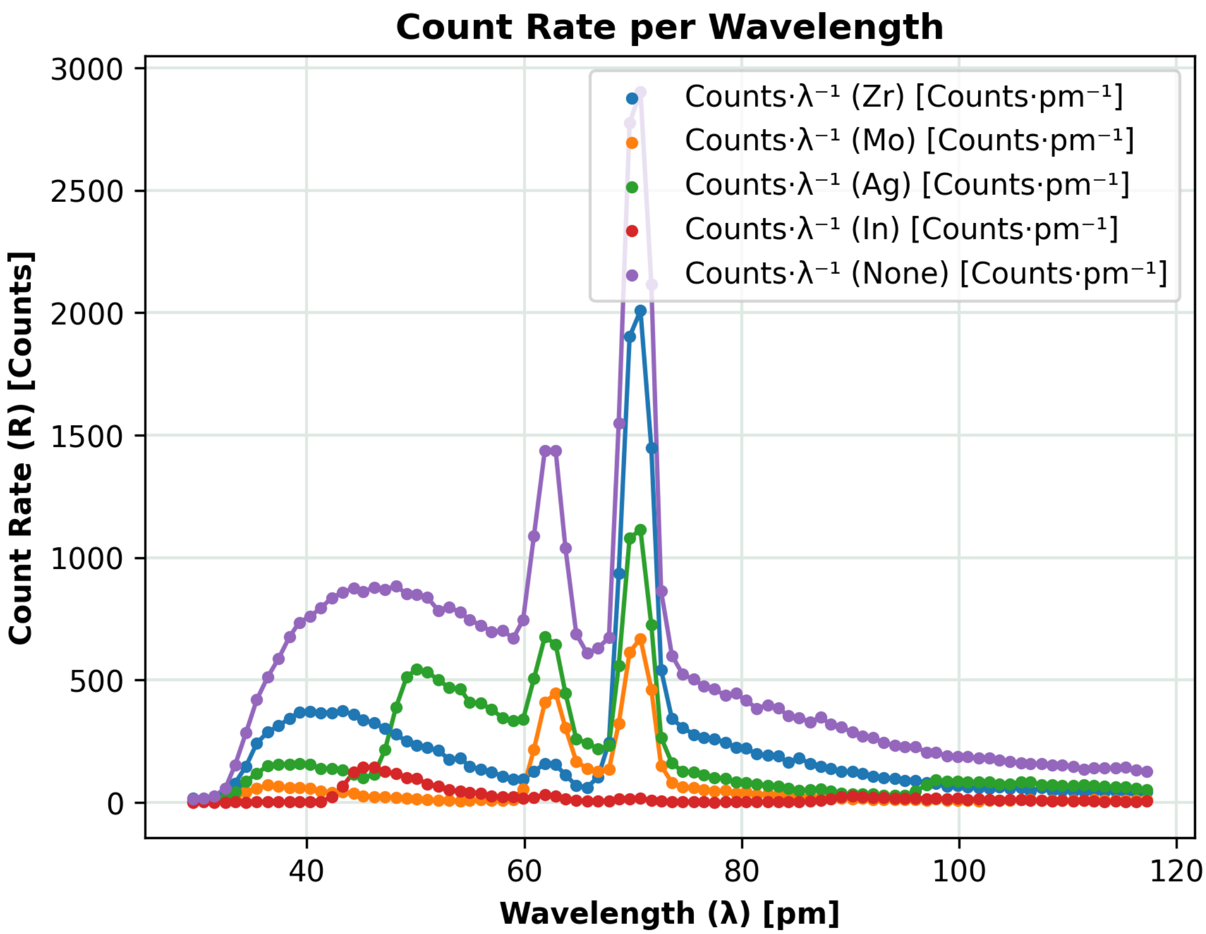

Figure 8: *Experiment 2, Section 1: Data*

Element	**K-Edge Wavelength** (λ_K) [$\pm$3 pm]	**K-Edge Transmittance** (T_K) [$\pm$0.5]
Zr	65	0.69
Mo	63	0.31
Ag	63	0.64
In	63	0.17

Table 2: Experiment 2 - Section 1: K-Edge Data

5.1.2 Experiment 2 - Section 2:

Element	**Prior to K-Edge Angle** (β_K^-) [± 0.05]	**Prior to K-Edge Wavelength** (λ_K^-) [± 0.5 pm]
Al	4.00	39.3
Fe	4.00	39.3
Ag	4.00	39.3
Zr	4.2	41.2

Table 3: Experiment 2 - Section 2: Prior to K-Edge Data

Element	**First Prior to K-Edge Count Rate** (R_{x_1}) [$\pm 0.5 s^{-1}$]	**Second Prior to K-Edge Count Rate** (R_{x_2}) [$\pm 0.5 s^{-1}$]
None (R_0)	133.2	129.0
Al	192.7	187.3
Fe	17.6	18.9
Ag	185.4	189.3
Zr	62.7	63.0

Table 4: Experiment 2 - Section 2:Prior to K-Edge Data

6 Results

6.1 Experiment 1:

Included below are the results for **Experiment 1**: The X-ray spectrum of molybdenum was successfully recorded at different accelerating voltages.

Minimum Wavelength (λ_{min}) [± 5 pm]	K_β **Transition Wavelength** (λ_{K_β}) [± 0.5 pm]	K_α **Transition Wavelength** (λ_{K_α}) [± 0.5 pm]
58	65	70
46	63	70
37	63	71
32	63	71

Table 5: Experiment 1: Wavelengths

The results below aligns with the theory which suggests that the product $U \cdot \lambda_{\text{min}}$ is a constant and the accepted value for Planck's constant is within the error of the estimates below:

$U \cdot \lambda_{\mathbf{min}}$ **Product** (λ_{max}) [$\pm 0.2\ \mu m \cdot V$]	**Planck's Constant** (h) [$\pm 10^{-34}\ J \cdot s^{-1}$]
1.2	6
1.2	6
1.1	6
1.1	6

Table 6: Experiment 1: Calculated Constants

The photon energies (and wavelength) lines of the K_α, and K_β in the characteristic spectrum of molybdenum were determined below and the theoretical values and the values found by Lawrence Berkeley National Laboratory were within the error range of the achieved values.

Maximum Energy ($E_{\max}$) [$\pm$3 keV]	K_β **Transition Energy** (E_{K_β}) [$\pm$3 keV]	K_α **Transition Energy** (E_{K_α}) [$\pm$3 keV]
21	19	17
27	20	17
33	20	17
38	20	17

Table 7: Experiment 1: Estimated Energies

6.1.1 Experiment 2 - Section 1:

Included below are the results for **Experiment 2 - Section 1**: The calculated transmittance per wavelength graph was almost entirely visually indistinct from the programme calculated transmittance per wavelength and their deviation was included in the error analysis section.

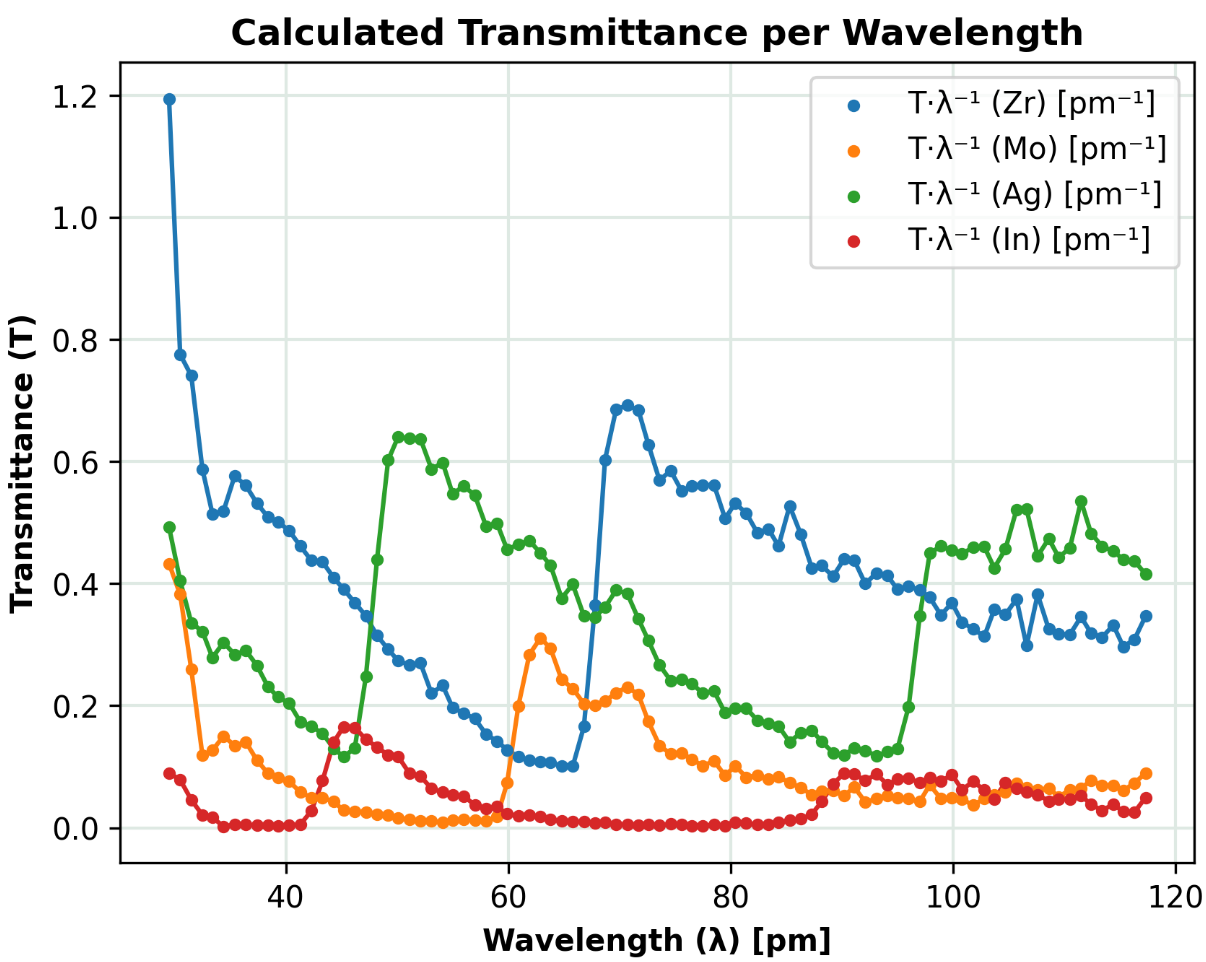

Figure 9: *Experiment 2, Section 1: Calculated Transmittance per Wavelength*

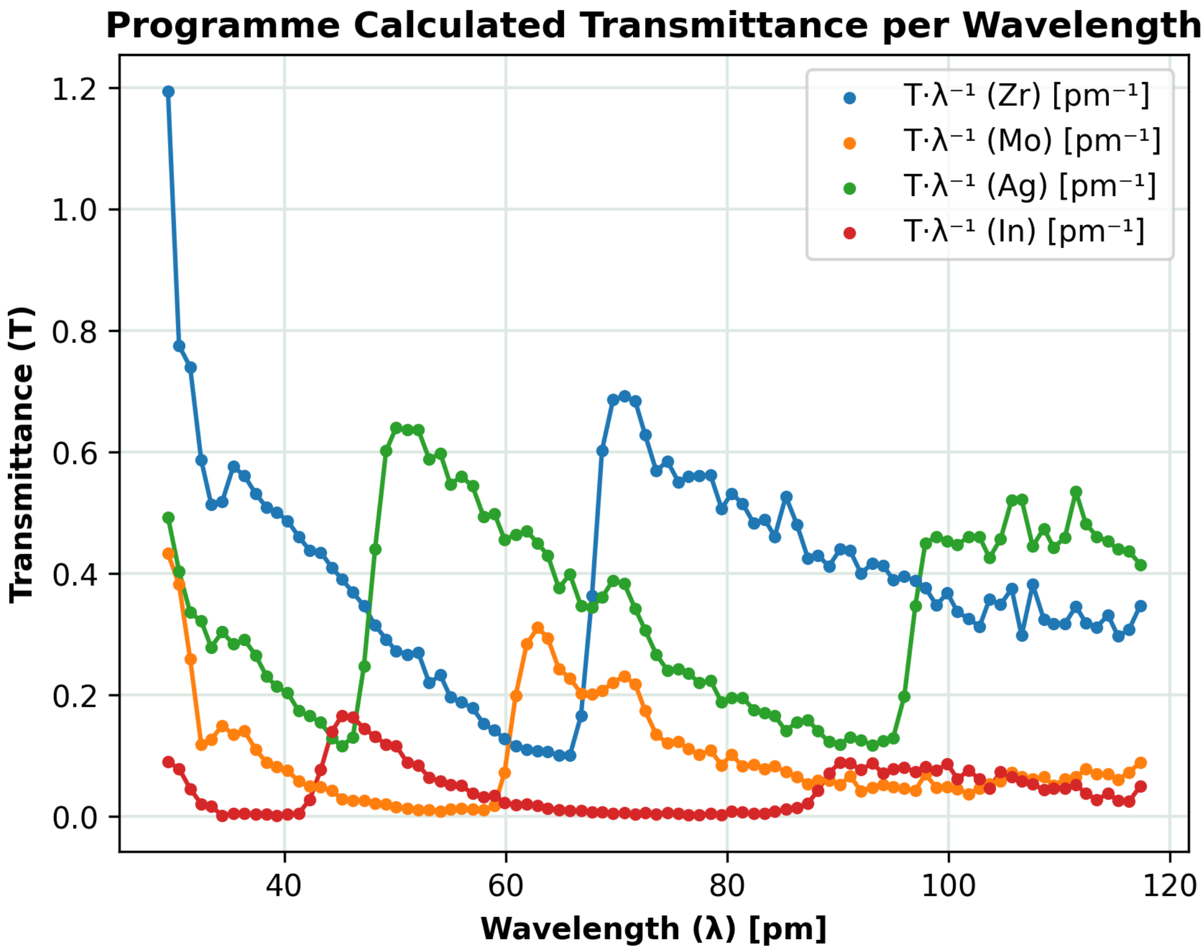

Figure 10: *Experiment 2, Section 1: Programme Calculated Transmittance per Wavelength*

The photon energy at the K-Edge E_{K} and associated removal cross-section σ_K was estimated as shown below:

Element	**K-Edge Energy** (E_{K}) [± 3 keV]	**K-Edge Removal Cross-Section** σ_K [$\pm 0.5\ A \cdot N_a^{-1}$]
Zr	17.5	1.1
Mo	19.7	1.2
Ag	24.8	0.9
In	27.6	0.8

Table 8: Experiment 2 - Section 1: K-Edge Calculated Values

The estimations asbove were used to demonstrate the proportionality posed by Mosely's law and the value of the Rydberg (R) constant was estimated as shown below:

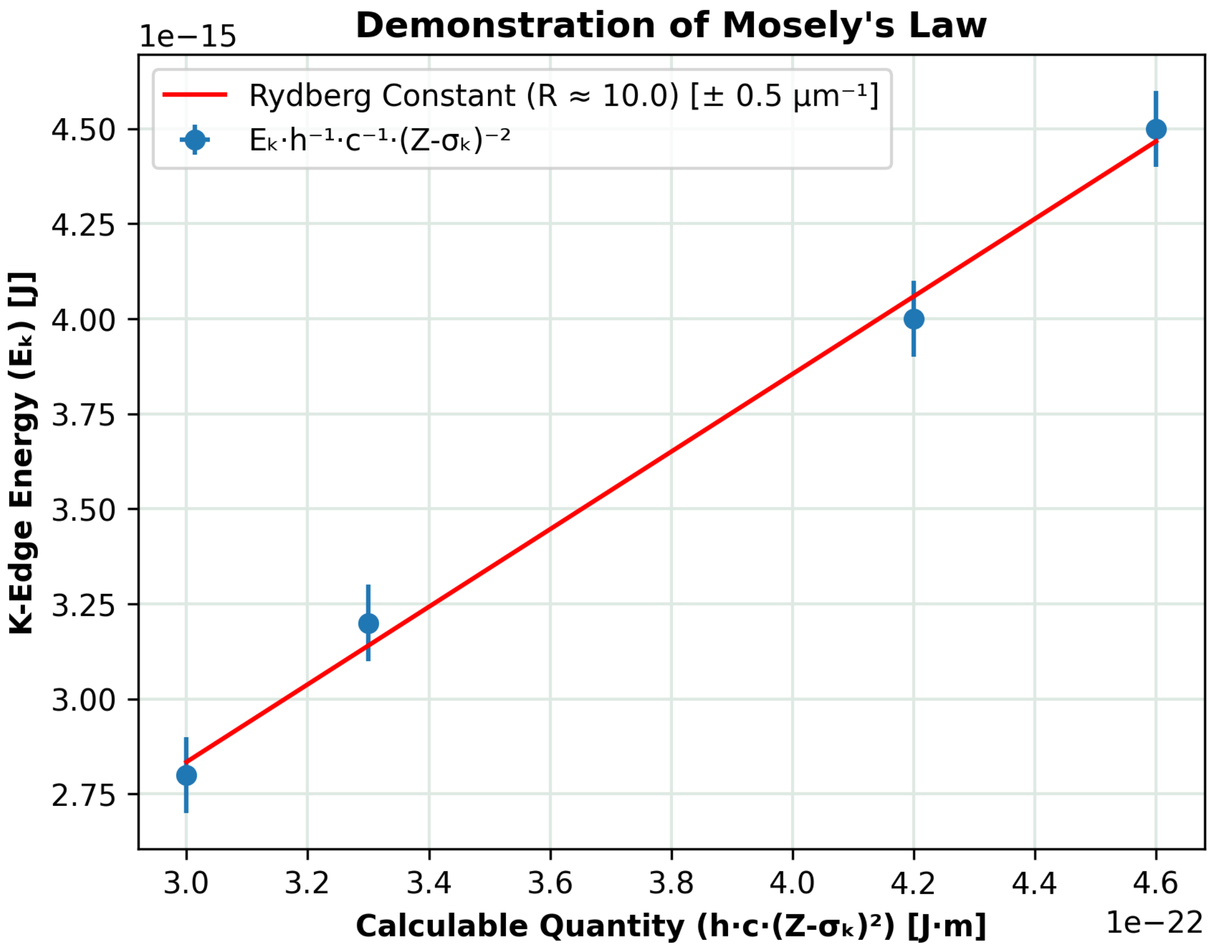

Figure 11: *Experiment 2, Section 1: Demonstration of Mosely's Law*

6.1.2 Experiment 2 - Section 2:

Element	First Prior to K-Edge Transmittance	Second Prior to K-Edge Transmittance	Average
	(T_1) $[\pm 0.5]$	(T_2) $[\pm 0.5]$	$(\overline{T})$ $[\pm 0.05]$
Al	1.4	1.5	1.45
Fe	0.1	0.2	0.15
Ag	1.4	1.5	1.45
Zr	0.5	0.5	0.5

Table 9: Experiment 2 - Section 2: Prior to K-Edge Calculated Transmittance

The prior to K-edge mass attenuation coefficient $\sigma \cdot \rho^{-1}$ and the prior to K-edge Absorption Cross-Section was estimated as shown below:

Element	Prior to K-Edge Mass Attenuation Coefficient $(\sigma \cdot \rho^{-1})$ $[A \cdot m^{-3} \cdot N_a^{-1} \cdot kg]$	Prior to K-Edge Absorption Cross-Section (σ_a) $[N_a^{-1} \cdot m^{-3}]$
Al	$2.8 \cdot 10^{-4}$	0.72
Fe	$-4.8 \cdot 10^{-4}$	-3.8
Ag	$7.1 \cdot 10^{-4}$	7.4
Zr	$-2.1 \cdot 10^{-4}$	-14

Table 10: Experiment 2 - Section 2: Prior to K-Edge Calculated Values

These values do not align with reality and seem to have fallen prey to experimental error.

7 Error Analysis and Propagation:

Error of the angle (β) was attributed based on whether or not the value was picked or discerned. The errors that were discerned were given greater values as it was selected based on data which had low signal to noise ratios.

Error propagation which required determining the error of a quotient was determined as demonstrated below:

$$\delta_T = \overline{T} \cdot \sqrt{(\frac{\delta_{R_0}}{\overline{R_0}})^2 + (\frac{\delta_R}{\overline{R}})^2} \tag{7.1}$$

Error propagation which required determining the error of a quantity which was averaged was determined as demonstrated below:

$$\delta_{\overline{T}} = \sqrt{\frac{\sum_{i=1}^{N} (T_i - \overline{T})^2}{N - 1}} \tag{7.2}$$

A plot of the deviation ($\sigma T \cdot \lambda^{-1}$) found between the Programme Calculated Transmittance per Wavelength and the computationally determined one for **Experiment 2: Section 1** is shown below:

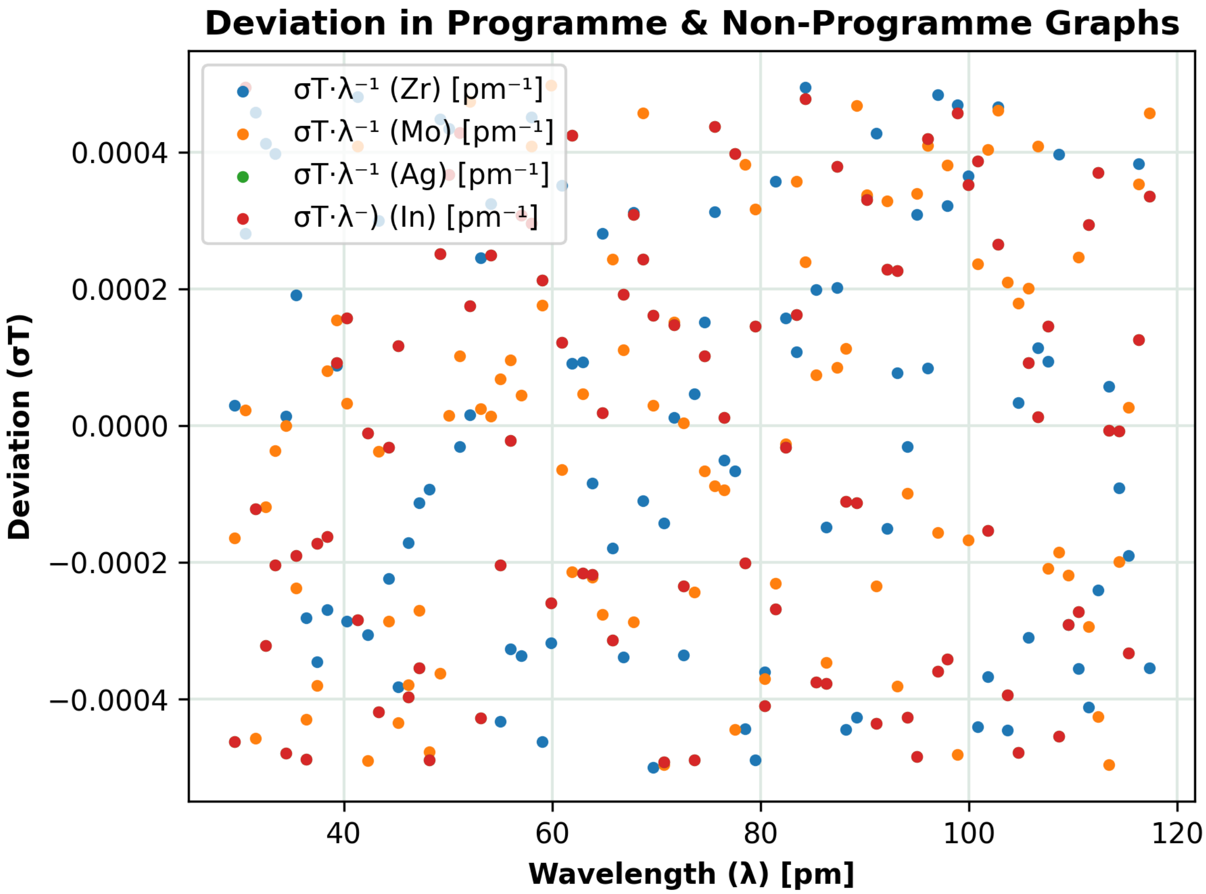

Figure 12: *Experiment 2, Section 1: Deviation Calculated vs Programme Calculated Transmittance per Wavelength*

The data found in **Experiment 2: Section 1** was found to not align with reality as the transmittance was found to be larger when the foil was covering the slit might be linked to the three separate major incidences the orientation of the NaCl crystal was incorrect during the conduction of this experiment which may require a re-evaluation of predicted error ranges.

8 Conclusions

The X-ray spectrum of molybdenum was successfully recorded at different accelerating voltages, revealing characteristic transitions such as K_α and K_β. The product $U \cdot \lambda_{\min}$ was found to be approximately constant, aligning with the expected theory. The estimated values for Planck's constant were in good agreement with the accepted value. Additionally, the K-edge energies of various metal foils were determined, confirming Mosley's Law. The absorption coefficients and mass attenuation coefficients for different materials were also calculated, demonstrating their dependence on atomic number Z. However the results for **Experiment 2 - Section 2** were unsuccesful. The aggregate of these results validate the effectiveness of X-ray spectroscopy in material analysis.

9 References / Bibliography:

Introduction to Solid State Physics. C. Kittel

X-Ray Data Booklet Lawrence Berkeley National Laboratory: Table 1-2. Photon energies, in electron volts, of principal K-, L-, and M-shell emission lines.
https://www.google.com/url?sa=t&source=web&rct=j&opi=89978449&url=
https://xdb.lbl.gov/Section1/Table_12.pdf
&ved=2ahUKEwjVo7vgwoEAxVPVEEAHV5WA0YQFnoECBkQAQ&usg=AOvVaw2qjBKbFcc45ydJn4wJMT
b %https://xdb.lbl.gov/Section1/Table_1-2.pdf

List of Figures